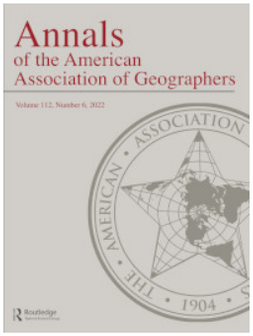

Annals of the American Association of Geographers

ISSN: (Print) (Online) Journal homepage: https://www.tandfonline.com/loi/raag21

Association between Global Air Pollution and COVID-19 Mortality: A Study of Forty-Six Cities in the World

Yuan Meng, Man Sing Wong, Mei-Po Kwan & Rui Zhu

To cite this article: Yuan Meng, Man Sing Wong, Mei-Po Kwan & Rui Zhu (2022) Association between Global Air Pollution and COVID-19 Mortality: A Study of Forty-Six Cities in the World, Annals of the American Association of Geographers, 112:6, 1777-1793, DOI: 10.1080/24694452.2022.2029342

To link to this article: https://doi.org/10.1080/24694452.2022.2029342

Published online: 04 Apr 2022.

Submit your article to this journal

Article views: 226

View related articles

View Crossmark data

Full Terms & Conditions of access and use can be found at
https://www.tandfonline.com/action/journalInformation?journalCode=raag21

Check for updates

Association between Global Air Pollution and COVID-19 Mortality: A Study of Forty-Six Cities in the World

Yuan Meng,[*] Man Sing Wong,[*,†] Mei-Po Kwan,[‡] and Rui Zhu[*]

[*]*Department of Land Surveying and Geo-Informatics, The Hong Kong Polytechnic University, Hong Kong, China*
[†]*Research Institute for Land and Space, The Hong Kong Polytechnic University, Hong Kong, China*
[‡]*Department of Geography and Resource Management and Institute of Space and Earth Information Science, The Chinese University of Hong Kong, Hong Kong, China*

Ambient air pollution plays a significant role in an increased risk of incidence and mortality of COVID-19 on a global scale. This study aims to understand the multiscale spatial effect of global air pollution on COVID-19 mortality. Based on forty-six cities from six countries worldwide between 1 April 2020 and 31 December 2020, a Bayesian space–time hierarchical model was used based on the lag effects of seven, fourteen, and twenty-one days to quantify the relative risks of NO_2 and $PM_{2.5}$ on the daily death rates of COVID-19, accounting for the effect of meteorological and human mobility variability based on global and city level. Results show that positive correlations between air pollution and COVID-19 mortality are observed, with the relative risks of NO_2 and $PM_{2.5}$ ranging from 1.006 to 1.014 and from 1.002 to 1.004 with the lag effects of seven, fourteen, and twenty-one days. For the individual city analysis, however, both positive and negative associations are found between air pollution and daily mortality, showing that the relative risks of NO_2 and $PM_{2.5}$ are between 0.754 and 1.245 and between 0.888 and 1.032, respectively. The discrepancies in air pollution risks among cities were demonstrated in this study and further allude to the necessity to explore the uncertainty in the multiscale air pollution–mortality relationship. *Key Words: air pollution, Bayesian space–time hierarchical model, COVID-19, multiscale analysis.*

Exposure to air pollution has been widely recognized to have a substantial impact on human health, including respiratory and cardiovascular disease (Brunekreef and Holgate 2002; Lelieveld et al. 2015). Rapid urbanization processes have resulted in various types of air pollution, including industrial air pollution from fossil fuel combustion, emissions from biomass burning such as nitrogen dioxide (NO_2), and fine particulate matter with a diameter less than 2.5 μm ($PM_{2.5}$; K. He, Huo, and Zhang 2002; Akimoto 2003). A study has projected a 50 percent increase in mortality corresponding to ambient air pollution by 2050 (Lelieveld et al. 2015), revealing the necessity of intensive air quality control measures on a global scale.

With the rapid emergence of COVID-19, the government-enforced policies, including lockdowns and social distancing measures, have drastically decreased socioeconomic activities and led to significant air pollution changes (Giani et al. 2020; G. He, Pan, and Tanaka 2020). An existing study has provided evidence that the lockdowns have caused a 60 percent and a 31 percent decline in NO_2 and $PM_{2.5}$, repectively, and an increasing trend in O_3 until 15 May 2020 in thirty-four countries (Venter et al. 2020). It provides an unprecedented opportunity to estimate the impact of air pollution counterfactual to business-as-usual situations on respiratory disease (i.e., COVID-19) on a global scale.

Among various air pollutants, NO_2 and $PM_{2.5}$, the major pollutants of anthropogenic emission, have been studied with the potential risks for the incidence and mortality of COVID-19. Villeneuve and Goldberg (2020) evaluated both tropospheric and ground-level NO_2 and $PM_{2.5}$ with daily or annual mean values based on varied time lag effects in different regions. Ogen (2020) focused on the satellite-based NO_2 distribution and analyzed its association with the fatality of COVID-19 in France, Germany, Italy, and Spain and further indicated the close relationship between long-term exposure to NO_2 and COVID-19 fatality. A study on China based on two-week confirmed cases of COVID-19 suggests that a 10 $\mu g/m^3$ increase in NO_2 and $PM_{2.5}$ is associated with 6.94 percent and 2.24 percent

Annals of the American Association of Geographers, 112(6) 2022, pp. 1777–1793 © 2022 by American Association of Geographers
Initial submission, November 2020; revised submissions, March, June, and October 2021; final acceptance, December 2021
Published by Taylor & Francis, LLC.

increases in the confirmed cases based on the lag effect of 0 to 14 (Zhu et al. 2020a). However, a study proposed by Gujral and Sinha (2021) shows a negative association between ground-based $PM_{2.5}$ and confirmed COVID-19 cases in Los Angeles, California, indicating the discrepancies of air pollution–COVID-19 incidences in different areas.

Other determinants of COVID-19 including meteorological and socioeconomic factors are required to be controlled when estimating the association of air pollution and COVID-19 incidence and mortality (Chowkwanyun and Reed 2020; Sarkodie and Owusu 2020; Yancy 2020; Kwok et al. 2021). Xie and Zhu (2020) adopted 122 cities from China within one month and revealed a positive linear relationship between mean temperature and the number of confirmed COVID-19 cases. In contrast, Shao, Xie, and Zhu (2021) suggested that on a global scale, ambient temperature is negatively associated with COVID-19 transmission mediated by human mobilities. Meteorological factors also include humidity and wind speed, in which a one-unit increase of absolute humidity corresponds to a decreasing trend of COVID-19 mortality in Wuhan, China (Ma et al. 2020), and cities with low wind speed, associated with atmospheric stability, had higher rates of COVID-19 incidence and mortality (Coccia 2021). Socioeconomic factors such as built environment, population, and human mobilities have also been considered in epidemiological modeling (Huang, Kwan, and Kan 2021; Kan et al. 2021; Oyedotun and Moonsammy 2021; Zhai et al. 2021). Existing research has revealed that higher betweenness centrality of transport nodes and population density in built-up regions are positively associated with COVID-19 infection ratios in China (Huang and Kwan 2021; S. Li, Ma, and Zhang 2021). Moreover, studies have estimated the COVID-19 infectious transmission by modeling human mobility patterns (Chang et al. 2021) and suggested the effectiveness of travel restrictions combined with transmission reduction interventions on mitigating the COVID-19 epidemic (Chinazzi et al. 2020).

Statistical models to estimate the association between air pollution and COVID-19 incidence and mortality vary among studies. Existing research has widely used Pearson correlation (Bashir et al. 2020), multiple linear regression (Andrée 2020; Coccia 2020; Barnett-Itzhaki and Levi 2021), difference-in-differences models (G. He, Pan, and Tanaka 2020; Ming et al. 2020), scenario analysis (Shan et al. 2021), generalized linear models (GLMs; Travaglio et al. 2021), and generalized additive models (GAMs; Prata, Rodrigues, and Bermejo 2020; Zhu et al. 2020b). Because these models were proposed in different areas with varied time lag effects, model comparisons based on the same spatiotemporal scales are required to assess their accuracies.

Despite the analysis of the different air pollution metrics, additional determinants including meteorological and human mobility factors, and varied statistical models that have been discussed, existing studies on COVID-19 incidence and mortality mainly focused on the city and country levels. Considering the pandemic transmission trends among countries, it is necessary to study a wider global perspective. Although several studies have investigated the global patterns of air pollution and COVID-19 epidemic variation (Forster et al. 2020; Le Quéré et al. 2020; Venter et al. 2020), lacking is a deeper understanding of the impact of the global trending air pollution mediated by meteorological and human mobility patterns. Moreover, the influence of multiscale spatial analysis should be considered to reduce the biases caused by constant spatial units. In addition, the performance of models that have been proposed in the association analysis needs to be evaluated to ensure model accuracy.

In this study, we focus on the association between air pollution and COVID-19 mortality on a global scale. Based on forty-six cities from six countries between 1 April 2020 and 31 December 2020, a Bayesian space–time hierarchical model (BSTHM) was used to estimate the impact of ground-based air pollution including NO_2 and $PM_{2.5}$ on COVID-19 mortality, controlling for the variables of meteorological factors and human mobility frequencies. The relative risks (RRs) of different air pollutants were estimated based on the overall global scale and spatial multiscale perspective. In addition, model comparisons were conducted to evaluate the effectiveness of the GLM, GAM, and BSTHM.

Materials and Methods

Study Area

Considering the data availability, including the exposure to air pollution and the corresponding COVID-19 deaths on a finer spatial level, we selected forty-six cities from six countries. Information collected consisted of high-quality air

Table 1. Selected countries and cities as study areas

Country	Cities and counties
Canada	Edmonton, Calgary, Ottawa, Toronto, Montreal
Germany	Berlin
China	Hong Kong
Mexico	Guadalajara, Monterrey
Netherlands	Amsterdam
United States	Ada, Alameda, Bernalillo, Clark, Cook, Dallas, Denver, District of Columbia, Duval, El Paso, Franklin, Fresno, Fulton, Harris, Hartford, Henrico, Hinds, King, Los Angeles, Maricopa, Marion, Milwaukee, Multnomah, New York City, Oklahoma, Philadelphia, Pima, Providence, Ramsey, Salt Lake, San Diego, San Francisco, Santa Clara, Suffolk, Wake, Wayne

station data, COVID-19 mortality data, and other controlling variables between 1 April and 31 December. As shown in Table 1, five cities from Canada, one city from Germany, one city from China, two cities from Mexico, one city from the Netherlands, and thirty-six cities and counties from the United States were selected as the study areas.

Air Pollution and Meteorological Data

Although data from satellites such as TROPOspheric Monitoring Instrument in Sentinel-5 Precursor show the potential to monitor spatiotemporal air pollution distribution on a global scale, the column concentration obtained from the satellite data cannot efficiently represent ground-level air pollutants. To fill this gap, this study adopted station-based air pollution and meteorological data from the Air Quality Open Data Platform (see https://aqicn.org/data-platform/covid19/). Specifically, daily air pollutants including NO_2 and $PM_{2.5}$ and daily meteorological data including daily humidity, pressure, temperature, and wind speed between 1 April and 31 December were collected from the selected cities. On this basis, missing values from the daily air pollution and meteorological data were further processed using the KalmanSmoother based on an autoregressive integrated moving average model (Bishop and Welch 2001).

Mobility Data from Apple

Human mobilities play a significant role in estimating epidemic disease transmission. To analyze the effect of human mobility patterns in different regions, daily mobility data were collected from the Apple Mobility Trends Reports (see https://covid19.apple.com/mobility). Specifically, the data calculate the comparative trip patterns for the report date to the baseline day (13 January 2020). The mobility data take 100 as the baseline, with the negative changes lower than 100 and the positive changes higher than 100. In this study, two types of transportation are considered: driving and walking. In addition, missing values in the temporal mobility data were filled using the autoregressive integrated moving average model.

Other Data as Controlling Variables

Four data sets, including accessibility to health care, the global friction surface, the NOAA Climate Data Record of Advanced Very High Resolution Radiometer (AVHRR) Normalized Difference Vegetation Index (NDVI), and the nighttime data from the Visible Infrared Imaging Radiometer Suite Day/Night Band (DNB) were adopted to distinguish additional physical and socioeconomic conditions among cities. In particular, accessibility to health care in the year 2019, which quantifies the land-based travel time to the nearest hospital or clinic, was averaged into a city scale. The global friction surface in 2019, enumerating the travel speed for all land pixels, which is considered a potential indicator for estimating COVID-19 transmission, was also averaged into the city scale. Both the accessibility to health care data set and the global friction surface data set were collected from the research proposed by Weiss et al. (2020). In addition, city-level averaged NDVI and DNB radiance values between 1

Table 2. Data sources of COVID-19 mortality in different countries

Country	Data sources
Canada	COVID-19 Canada Open Data Working Group (https://github.com/ccodwg/Covid19Canada)
Germany	Das Datenportal für Deutschland (https://www.govdata.de)
China	Data.gov.hk (https://data.gov.hk/en-data/dataset/hk-dh-chpsebcddr-novel-infectious-agent)
Mexico	Covid-19 México (https://datos.covid-19.conacyt.mx/#DownZCSV)
Netherlands	Dataregister van de Nederlandse Overheid (https://data.overheid.nl)
United States	*The New York Times* (https://github.com/nytimes/covid-19-data)

April and 31 December were calculated separately from the NOAA Climate Data Record of AVHRR NDVI and Visible Infrared Imaging Radiometer Suite DNB nighttime data. In addition, the global population in 2019 was collected from LandScan (see https://landscan.ornl.gov) as the offset variable in the statistical analysis in the following section.

COVID-19 Data

The COVID-19 mortality data from forty-six cities between 1 April and 31 December were collected from multiple sources, which are displayed in Table 2. The daily deaths were calculated based on the total deaths provided in the COVID-19 data.

Statistical Models

The BSTHM, made up of the hierarchical Bayesian model and the space–time interaction model, consists of three components: the overall spatial, temporal, and space–time interaction. It has been commonly applied in many fields such as public health (Knorr-Held 2000; Richardson, Abellan, and Best 2006; Liao et al. 2016), population assessment (Wang et al. 2021), and air pollution modeling (J. Li, J. Wang et al. 2018; J. Li, N. Wang et al. 2018). Compared with other statistical models such as the GLM and GAM, hierarchical Bayesian models accommodate unobserved values and prior probability distributions to improve estimation accuracies (Dunson 2001).

Specifically, we assume that y_{it} is the deaths in the city $i = (1, 2, \ldots, N)$ at the time point $t = (1, 2, \ldots, T)$, the number of daily deaths can be modeled by the Poisson regression with the log link function

$$y_{it} \sim Poisson(n_i r_{it}), \tag{1}$$

where n_i indicates the base distribution in city i, and r_{it} represents the underlying mortality risk, which can be further modeled as follows:

$$\begin{aligned}\log(r_{it}) = {} & \alpha + \theta_i + \delta_t + \gamma_{it} + \beta_{no2} x_{it,no2} + \beta_{pm25} x_{it,pm25} \\ & + \beta_{humi} x_{it,humi} + \beta_{pres} x_{it,pres} + \beta_{temp} x_{it,temp} \\ & + \beta_{wind} x_{it,wind} + \beta_{driving} x_{it,driving} \\ & + \beta_{walking} x_{it,walking} + \beta_{acce} x_{i,acce} + \beta_{fric} x_{i,fric} \\ & + \beta_{NDVI} x_{i,NDVI} + \beta_{night} x_{i,night} + \log(x_{i,pop}) \\ & + \varepsilon_{it}\end{aligned} \tag{2}$$

in which β_{no2}, β_{pm25}, β_{humi}, β_{pres}, β_{temp}, β_{wind}, $\beta_{driving}$, $\beta_{walking}$, β_{acce}, β_{fric}, β_{NDVI}, and β_{night} refer to the regression coefficients of daily NO_2, $PM_{2.5}$, humidity, pressure, mean temperature, mean wind speed, and the daily trip based on driving and walking transportation, accessibility to health care, the degree of friction, NDVI, and the DNB radiance values with the following prior distributions $\pi(\cdot)$ assigned to the coefficients:

$$\pi(\beta) = \mathrm{N}(0, 1000). \tag{3}$$

In addition, α indicates the sum of the intercept. θ_i, δ_t, and γ_{it} refer to the spatial main effect, temporal main effect, and space–time interaction, respectively. $\log(x_{i,pop})$ represents the offset variable based on the total population in each region. ε_{it} is the additional residual term. Moreover, the seven-, fourteen-, and twenty-one-day lag effects of socioeconomic and environmental factors on COVID-19 mortality are considered.

Prior distributions are further assigned to the preceding parameters. The Besag–York–Mollié model is employed to the spatial main effect, temporal main effect θ_i and δ_t, in which the Besag–York–Mollié model is a convolution of a spatially structured and spatially unstructured random effect (Besag, York, and Mollié 1991). Specifically, the spatial structure is applied by the conditional autoregressive models. The priors of θ_i, δ_t, and γ_{it} are modeled as follows:

$$\theta_i|\boldsymbol{\theta}_{-i}, \mathbf{W} \sim N\left(\frac{\rho_s \sum_{j=1}^{N} w_{ij}\theta_j}{\rho_s \sum_{j=1}^{N} w_{ij} + 1 - \rho_s}, \frac{\tau_s^2}{\rho_s \sum_{j=1}^{N} w_{ij} + 1 - \rho_s}\right) \quad (4)$$

$$\delta_t|\boldsymbol{\delta}_{-t}, \boldsymbol{D} \sim N\left(\frac{\rho_t \sum_{j=1}^{T} d_{ij}\delta_j}{\rho_t \sum_{j=1}^{T} d_{ij} + 1 - \rho_t}, \frac{\tau_t^2}{\rho_t \sum_{j=1}^{T} d_{ij} + 1 - \rho_t}\right) \quad (5)$$

$$\gamma_{it} \sim N\left(0, \tau_k^2\right), \quad (6)$$

where $\mathbf{W} = (w_{ij})$ and $\boldsymbol{D} = (d_{tj})$ represent the neighborhood matrix and the time adjacency, respectively, and $w_{ij} = 1$ and $d_{tj} = 1$ if areas (i, j) share a common border and time $|j - t| = 1$; otherwise, $w_{ij} = 0$ and $d_{tj} = 0$. (ρ_s, ρ_t) and (τ_s, τ_t, τ_k) refer to the parameters of the fixed uniform and inverse-gamma distribution, respectively, the prior of which is modeled as

$$\rho_s, \rho_t \sim \text{Uniform}(0, 1) \quad (7)$$

$$\tau_s, \tau_t, \tau_k \sim \text{Inverse} - \text{Gamma}(1, 0.01). \quad (8)$$

Specifically, the neighborhood matrix is constructed based on the spatial distribution among cities, with $w_{ij} = 1$ among each pair of adjacent cities and $w_{ij} = 0$ otherwise.

The proposed BSTHM was implemented the Markov chain Monte Carlo method and Gibbs sampling. Air pollutants including daily NO_2 and $PM_{2.5}$ are used for estimating the number of deaths, and meteorological factors, human mobilities, population, and other factors are considered as controlled variables. The collinearity of variables was assessed using the variance inflation factor. Then, the estimated RR, which is proposed based on the exponential transformation of the modeling coefficients, was calculated to estimate the impact of air pollutants on the changes in COVID-19 mortality.

Results

Descriptive Analysis

Table 3 shows the statistics for the daily deaths from COVID-19, air pollutants, meteorological factors, human mobility, population, and other controlling variables in each city. Number of daily deaths varies from 0 to 1,221, and daily NO_2 and $PM_{2.5}$ are 7.186 ppb and 33.783 $\mu g/m^3$, respectively. The mean daily humidity, pressure, temperature, and wind speed are 62.708 percent, 1,011.274 mb, 17.018 °C, and 2.687 m/s, respectively. For urban mobility, the daily changes of driving and walking transportation are 103.482 and 110.176, respectively. In addition, the average values of accessibility to health care, the degree of friction, NDVI, and nighttime radiance are 12.191, 0.004, 1,652.558, and 18.484, respectively.

Table 3. Summary of the ground station data, meteorological data, mobility data, other controlling variables, and COVID-19 mortality

Variables	Daily measures				
	Minimum	Maximum	M	*SD*	Variance
Daily deaths	0	1,221	7.63	33.481	1,120.971
Air pollutant					
NO_2 (ppb)	0.100	49.100	7.186	5.324	28.349
$PM_{2.5}$ ($\mu g/m^3$)	0.000	404.000	33.783	21.117	445.942
Meteorological factors					
Humidity (%)	0.000	100.000	62.708	21.740	472.630
Pressure (mb)	415.400	1,039.500	1,011.274	26.257	689.446
Temperature (°C)	−17.700	39.200	17.018	8.710	75.867
Wind speed (m/s)	0.034	17.000	2.687	1.630	2.657
Human mobility					
Driving	22.390	209.340	103.482	30.682	941.367
Walking	7.870	295.690	110.176	45.153	2,038.763
Population	2.471E + 05	1.008E + 07	2.037E + 06	2.041E + 06	4.164E + 12
Other controlling variables					
Accessibility to health care	1.597	47.056	12.191	11.282	127.274
Friction	0.001	0.013	0.004	0.003	0.000
NDVI	953.004	2,435.288	1,652.558	399.947	159,957.745
Nighttime radiance	1.136	49.768	18.484	13.317	177.333

Note: NDVI = Normalized Difference Vegetation Index.

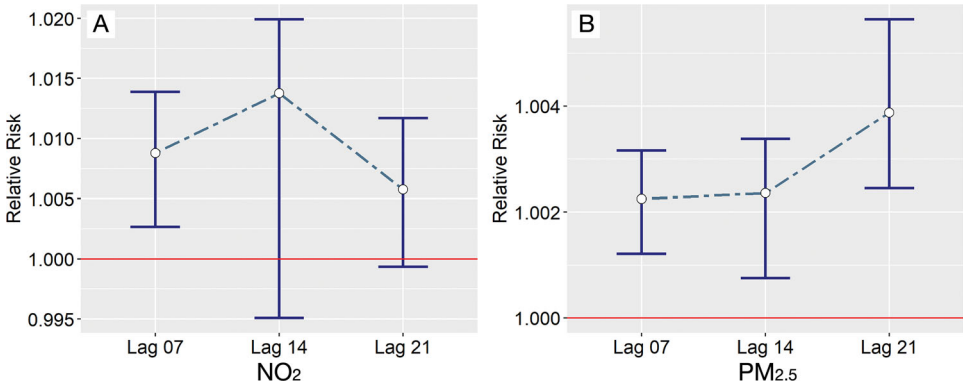

Figure 1. Relative risk (with 95 percent confidence interval) of (A) NO_2 and (B) $PM_{2.5}$ on COVID-19 mortality with different time lag effects.

Overall BSTHM Results

Figure 1 shows the RR with a 95 percent credible interval of air pollutants with the COVID-19 mortality with time lag of seven, fourteen, and twenty-one days. In summary, the increasing values of NO_2 and $PM_{2.5}$ are positively correlated with COVID-19 mortality, indicating increasing daily deaths with higher NO_2 and $PM_{2.5}$ exposure. It is reasonable that both NO_2 and $PM_{2.5}$ and COVID-19 mortality have a positive association because a decrease in NO_2 and $PM_{2.5}$ has been demonstrated to reduce respiratory mortality in other studies (Di et al. 2017; Liu et al. 2019; Khomenko et al. 2021). In addition, the association between NO_2, $PM_{2.5}$, and COVID-19 mortality varies according to the different time lag effects.

In particular, the RR of a 1 ppb increase in NO_2 with a seven-day lag effect is 1.009 (confidence interval [CI] [1.003, 1.014]). For the lag effect of fourteen days, the RR is 1.014 (CI [1.014, 1.020]), which is approximately 0.5 percent higher than the RR based on the seven-day lag effect. Meanwhile, the RR of NO_2 with a twenty-one-day lag effect is 1.006 (CI [0.999, 1.012]), which is 0.3 percent and 0.8 percent lower than those of seven- and twenty-one-day lag effects. For the RR of $PM_{2.5}$, similar patterns are revealed with the lag effects of seven and fourteen days, representing approximately a 0.2 percent increase (CI [1.001, 1.003]) in daily deaths with a 1 $\mu g/m^3$ increase in $PM_{2.5}$. Changes are revealed in the lag effect of twenty-one days, showing the RR of 1.004 (CI [1.002, 1.006]), approximately 0.2 percent higher than the RRs based on seven- and fourteen-day lag effects.

Despite the varied lag effects (the association analysis without time lag effects is excluded considering the incubation period of COVID-19), the results indicate that higher exposures to NO_2 and $PM_{2.5}$ are estimated to increase the risks of COVID-19 mortality from the perspective of global cities. Because this study was conducted between 1 April and 31 December, the potential influence of lockdown and restricted social distancing policies was considered, measured by human mobility data. On the other hand, because public vaccination started at the end of 2020 (Mathieu et al. 2021), its impacts on COVID-19 mortality are not discussed in this study. Because the proposed controlling variables in BSTHM might not completely depict the environmental and socioeconomic conditions of individual cities, the discrepancies of RRs among cities are not discussed. To fill this gap, the air pollution–mortality association analysis is proposed in the following section.

City-Level Analysis

Changes in the study areas show a significant impact on the air pollution–COVID-19 mortality analysis. After analyzing the overall impacts of NO_2 and $PM_{2.5}$ on COVID-19 mortality based on all of the selected cities, we further focus on the RRs of individual cities separately. The air pollution–COVID-19 mortality association of each city was estimated using Bayesian hierarchical modeling. Because no spatial adjacency issue was found in individual cities, the spatial effect was removed from the proposed models.

Figure 2 shows the RRs of NO_2 with time lag effects of seven, fourteen, and twenty-one days of individual cities. In summary, the RRs of NO_2 exposure vary among cities. Despite the different time lag

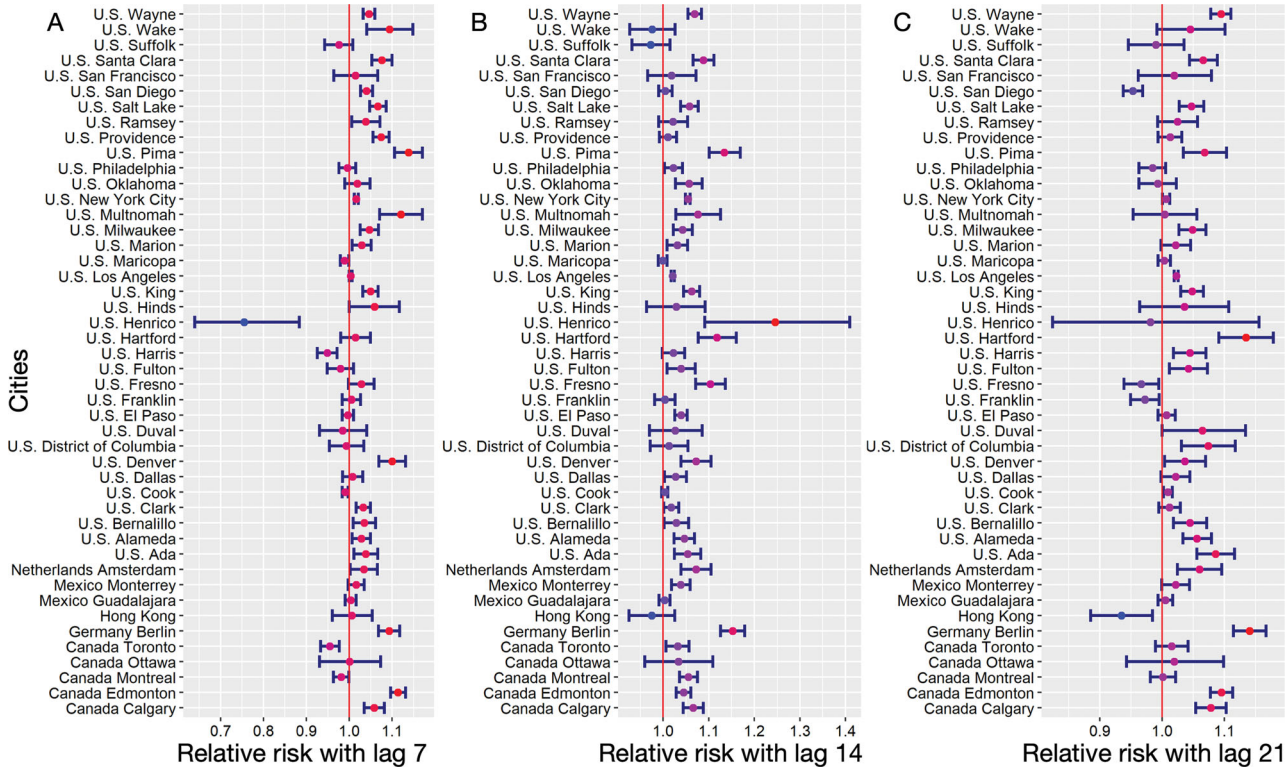

Figure 2. Relative risk (with 95 percent confidence interval) of NO_2 with time lag effects of (A) seven days, (B) fourteen days, and (C) twenty-one days at the city scale.

effects, most of the cities show a positive impact of NO_2–COVID-19 mortality association. It should be noted that significant discrepancies of relative risks are revealed among Henrico in the United States and other cities, showing a large range of CIs based on all lag effects, with dramatically lower and higher RRs based on seven- and fourteen-day lag effects, respectively. No significant differences in RRs are revealed among other cities for the lag effects of seven, fourteen, and twenty-one days, within values between 0.948 and 1.138, between 0.973 and 1.152, and between 0.935 and 1.141. The results, however, still revealed a negative association between NO_2 and COVID-19 mortality in many cities, such as the RRs based on fourteen- and twenty-one-day lag effects in Hong Kong in China and fourteen-day lag effect–based RRs in Suffolk and Wake in the United States. Further explanations of the negative trends are discussed later in this section.

The RRs of $PM_{2.5}$ on the daily death rates of COVID-19 are shown in Figure 3. The estimated RRs based on seven-, fourteen-, and twenty-one-day effects range between 0.887 and 1.032, between 0.968 and 1.013, and between 0.971 and 1.023, respectively. As with the RRs of NO_2, no significant changes are shown in most of the cities. Anomalies are observed, however, indicating significant discrepancies or negative trends, in several cities, such as the seven-day lag effect–based RR in Providence and Pima in the United States and Edmonton and Calgary in Canada; a fourteen-day lag effect–based RR in Hong Kong and Pima, Henrico, and Hartford in the United States; and a twenty-one-day lag effect–based RR in Calgary and Edmonton in Canada, Hong Kong in China, and Pima in the United States.

The question of how to interpret these anomalies in the RRs is important in the air pollution evaluation, especially the anthropogenic emissions. To solve this issue, deeper investigation on daily deaths, NO_2 and $PM_{2.5}$ emission, and human mobility for individual cities is proposed. Because the number of deaths could influence the RR estimation (a smaller number of daily deaths, such as zero deaths per day, could lead to estimation biases), the total deaths from COVID-19 from 1 April to 31 December in individual cities were calculated. As

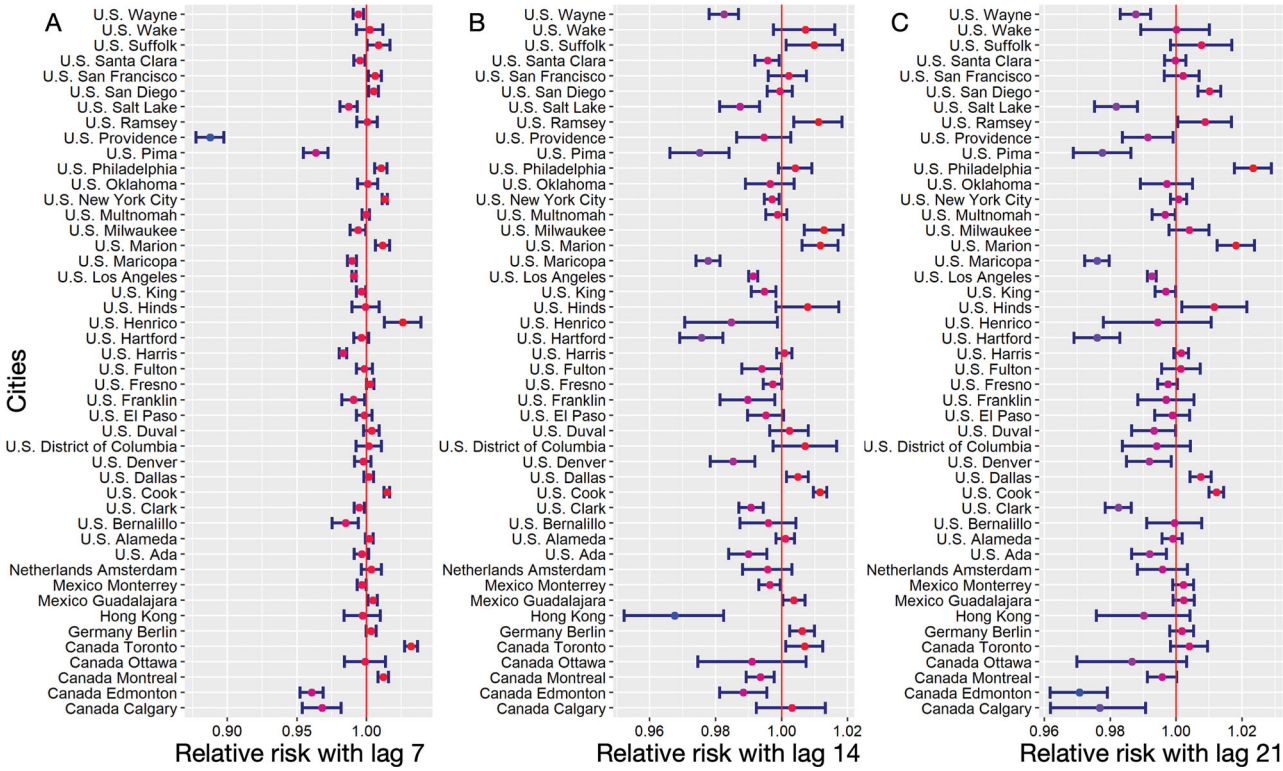

Figure 3. Relative risk (with 95 percent confidence interval) of $PM_{2.5}$ with time lag effects of (A) seven days, (B) fourteen days, and (C) twenty-one days at the city scale.

displayed in Figure 4, a small number of total deaths are found in cities such as Hong Kong in China; Calgary and Ottawa in Canada; and Hinds, Henrico, Multnomah, and Salt Lake in the United States, with the total number of deaths lower than 600. It is consistent with the RR biases that the impacts of NO_2 are dramatically lower and higher with seven- and fourteen-day lag effects with a large range of CIs in Henrico in the United States, as well as the negative RR in Salt Lake in the United States. The small number of deaths also provides hints in evaluating the RR biases of $PM_{2.5}$, suggesting that the smaller number of deaths might cause the significant negative RRs in Hong Kong in China, Calgary and Ottawa in Canada, and Multnomah in the United States. In summary, the potential impact of air pollution could be estimated with significant biases faced with a smaller number of daily deaths. There are also other potential factors, however, that could influence the RR estimation.

As with the small number of deaths, the level of air pollution plays a dominant role in evaluating the potential risks of air pollution in different cities (Chen et al. 2012). Figure 5 displays the average daily emissions of NO_2 and $PM_{2.5}$ from 1 April to 31 December in each city. Several cities with lower levels of NO_2 and $PM_{2.5}$ reported anomalies in RR estimation. For example, Henrico in the United States, with average daily NO_2 emissions lower than 2 ppb, shows significant negative trends in evaluating the RRs of NO_2 on COVID-19 mortality. The lower emissions of $PM_{2.5}$ in Calgary and Edmonton in Canada, which are approximately 20 $\mu g/m^3$, also provide evidence on the biases of RR estimation. Although lower level air pollution could reduce the impact of NO_2 and $PM_{2.5}$ on mortality assessment, leading to biases in RR estimation, no evidence has been provided about whether different air pollution levels are significantly correlated with the accuracies of potential risk estimation on cause-specific mortality.

Our analysis has also considered the levels of human activity restriction to assess the role of anthropogenic emissions. Generally, the decrease in driving trips could reduce anthropogenic emissions (Meng et al. 2021), and the lower level walking activities show the potential to reduce the risk of virus transmission (Chu et al. 2020). This study proposed a mobility variation index to measure the

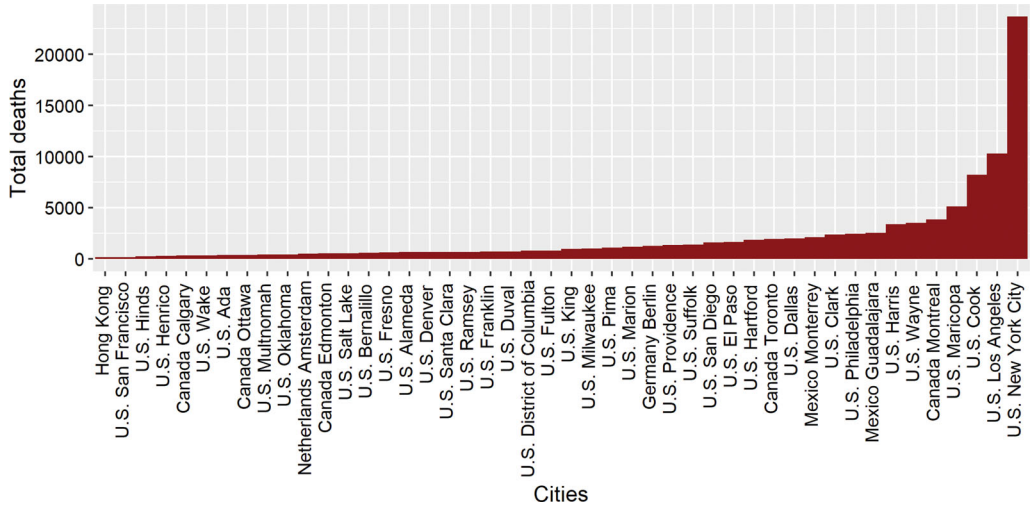

Figure 4. Total deaths from COVID-19 between 1 April 2020 and 31 December 2020 in individual cities.

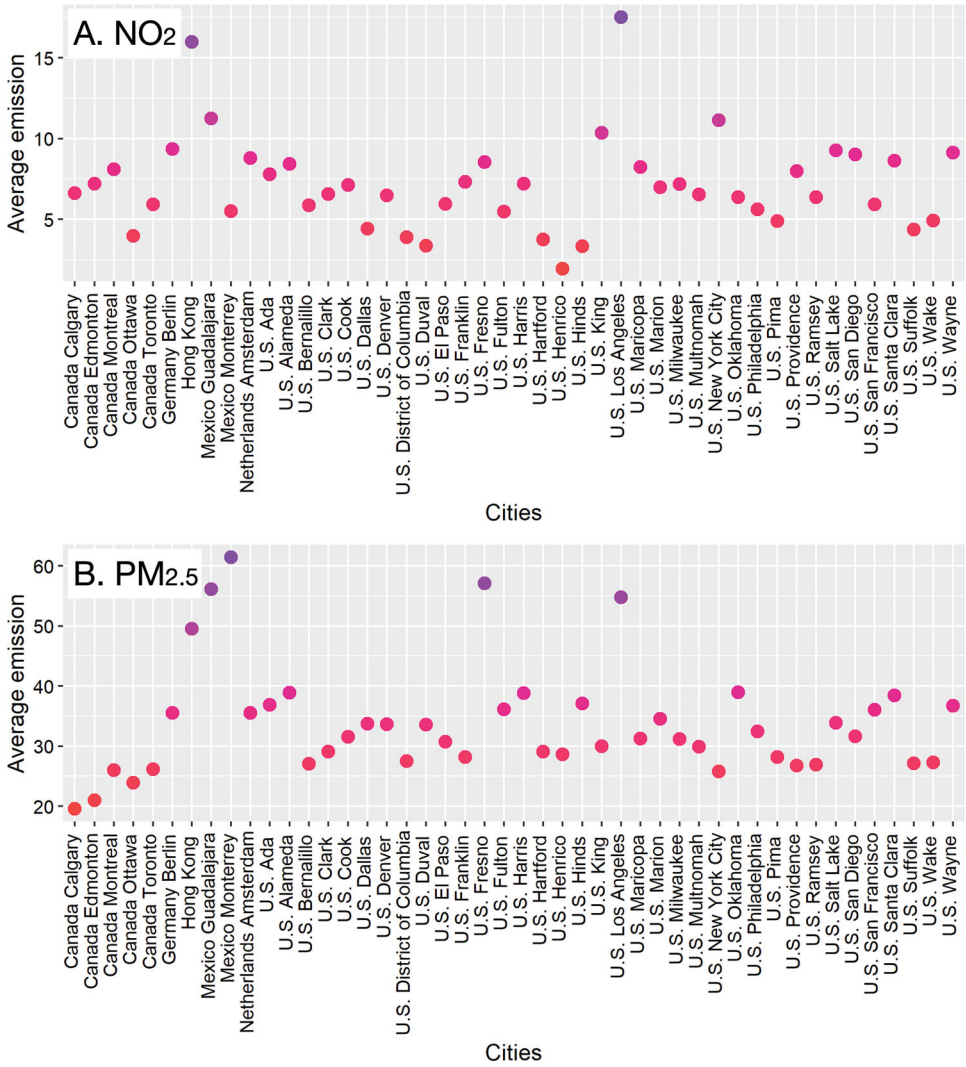

Figure 5. Average (A) NO_2 and (B) $PM_{2.5}$ emission between 1 April 2020 and 31 December 2020 of individual cities.

overall trends and changes of driving and walking transportation in each city using the Apple mobility data:

$$MV_i = \begin{cases} \sqrt{\dfrac{Mobility_{max,i} - \sum_{d=1}^{n} Mobility_{i,d}/n}{\left(\sum_{d=1}^{n} Mobility_{i,d}/n\right)^2}}, & \sum_{d=1}^{n} Mobility_{i,d} \geq 0 \\ -\sqrt{\dfrac{\left|Mobility_{min,i}\right| - \left|\sum_{d=1}^{n} Mobility_{i,d}/n\right|}{\left(\sum_{d=1}^{n} Mobility_{i,d}/n\right)^2}}, & \sum_{d=1}^{n} Mobility_{i,d} < 0, \end{cases} \quad (9)$$

where MV_i represents the quantified mobility variation of the ith city. $Mobility_{max,i}$ and $Mobility_{min,i}$ indicate the maximum and minimum values of daily mobility changes, respectively, which are calculated from the daily mobility data represented by the Apple Mobility Trends Reports. Because the mobility data take 100 as the baseline, the changes in mobility are scaled to a baseline as 0, with mobility higher and lower than 0 indicating positive and negative mobility variation, respectively. $Mobility_{i,d}$ refers to the mobility change of the ith city on the dth day. Specifically, positive and negative values represent the overall increase and decrease in human activity patterns, with the higher absolute values (regardless of the positive or negative directions) showing a higher degree of activity changes.

The calculated mobility variations for driving and walking in forty-six cities are shown in Figure 6. For driving, Maricopa in the United States reported the highest level of decreasing activities with the value of approximately −0.563, whereas Pima in the United States showed the largest increase of driving trips (0.408). This indicates that the proposed policies during COVID-19 yielded a significant influence on driving transportation, especially the activity changes during and after the short-term restricted social distancing policies. For the variation in walking transportation, Maricopa in the United States still reported the highest level of decreasing activities, with a reduction of walking trips of about −0.463. In addition, Alameda in the United States reported the largest increase in walking transportation, with a mobility variation index of approximately 0.357. Those discrepancies in driving and walking transportation among cities are significant for assessing the potential risks of air pollution. For example, the decrease of driving and walking activities in Maricopa in the United States could reduce the emission of $PM_{2.5}$, leading to the biases of a negative association with daily deaths based on the lag effects of seven, fourteen, and twenty-one days.

In summary, the air pollution–COVID-19 mortality analysis shows discrepancies among individual cities. Influenced by the number of deaths, air pollution conditions, and the degree of human mobility variation, biases (usually the negative impact of air pollution) exist in evaluating the RRs of NO_2 and $PM_{2.5}$ in several cities, such as Henrico and Pima in the United States, Hong Kong in China, and Calgary in Canada. The negative trends of RRs in terms of $PM_{2.5}$ in several cities cannot be explained in this section, such as Providence and Wayne in the United States, which are further discussed in the following sections.

Model Assessment

To evaluate the accuracy of BSTHM, comparative studies were proposed by involving GLMs and GAMs. Specifically, GLMs and GAMs with negative binomials were used to estimate the association between air pollution with time lag effects (seven-, fourteen-, and twenty-one-day lags) and COVID-19 mortality. Spatial fixed effects and time fixed effects are included to control spatial and temporal characteristics. For the implementation of GAMs, the degrees of freedom, which are applied for the controlling variables including meteorological and human mobility factors, were selected using the generalized cross-validation criterion.

The performance of the proposed models, including GLM, GAM, and BSTHM, was evaluated by calculating the root mean square errors (RMSEs). Specifically, RMSE calculates the standard deviation

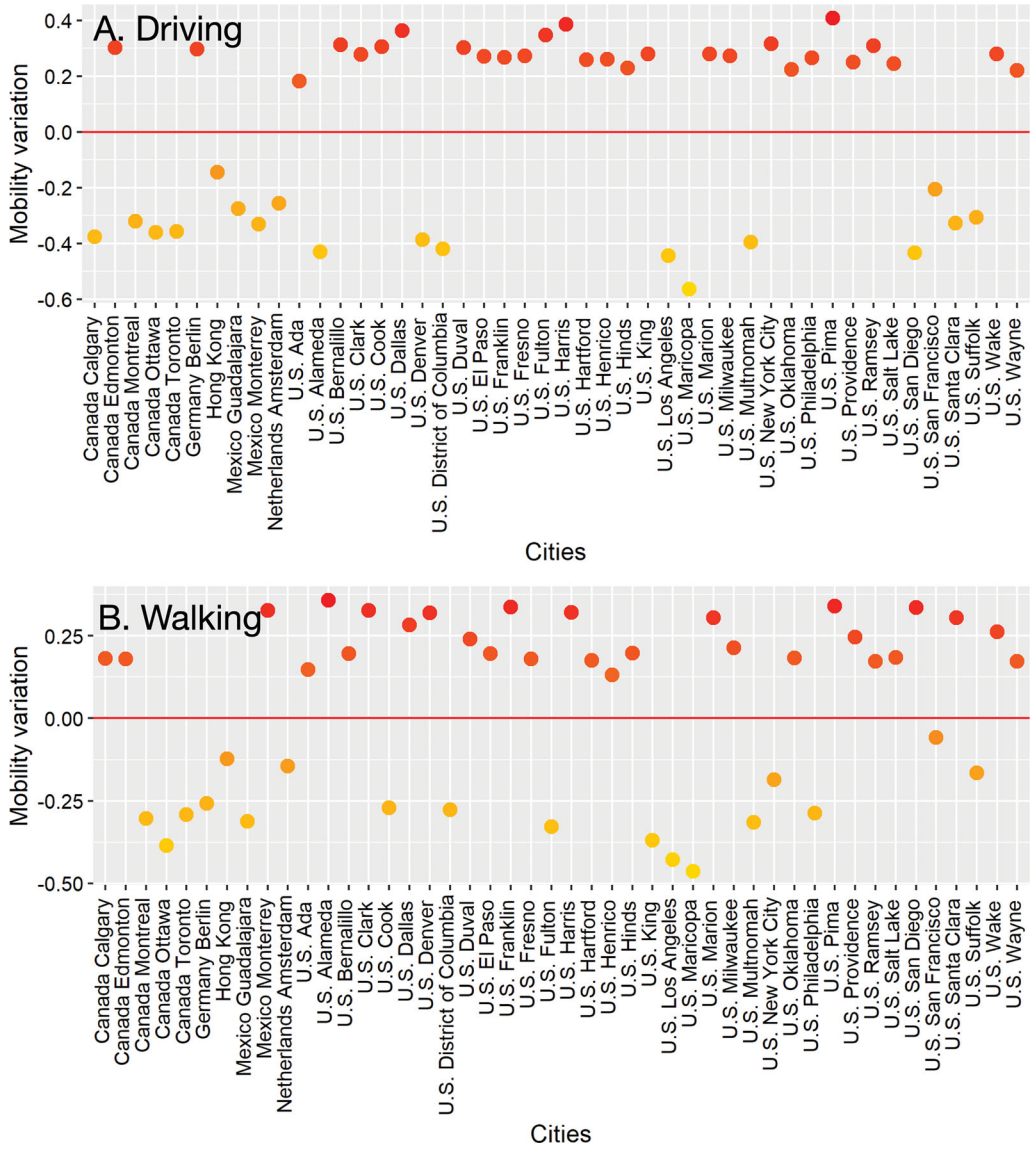

Figure 6. Mobility variation of (A) driving and (B) walking transportation between 1 April 2020 and 31 December of individual cities.

of the prediction error. As shown in Table 4, the RMSEs of the GLM for the seven-, fourteen-, and twenty-one-day lags are 25.181, 21.509, and 15.460, respectively. The RMSEs of the GAM are 24.317, 19.629, and 15.328, respectively. For the BSTHM proposed in this study, the RMSEs for the seven-, fourteen-, and twenty-one-day lags are 0.703, 0.721, and 0.726, respectively. This indicates that BSTHM achieves better performance than GLM and GAM. Note, however, that although a lower value of RMSE represents better model performance, it could also lead to an overfitting issue. Because we focus on the overall trends of model regression instead of classification, the biases caused by the potential overfitting problem could be reduced. On this basis, the overall RRs of NO_2 and $PM_{2.5}$ were further estimated and compared among GLM, GAM, and BSTHM.

Table 4. Root mean square error calculated from GLM, GAM, and BSTHM models with different lag effects

Model	Lag 7	Lag 14	Lag 21
GLM	25.181	21.509	15.460
GAM	24.317	19.629	15.328
BSTHM	0.703	0.721	0.726

Note: GLM = generalized linear model; GAM = generalized additive model; BSTHM = Bayesian space–time hierarchical model.

Figure 7 shows the RR of NO_2 and $PM_{2.5}$ with a 95 percent CI based on GLM, GAM, and BSTHM.

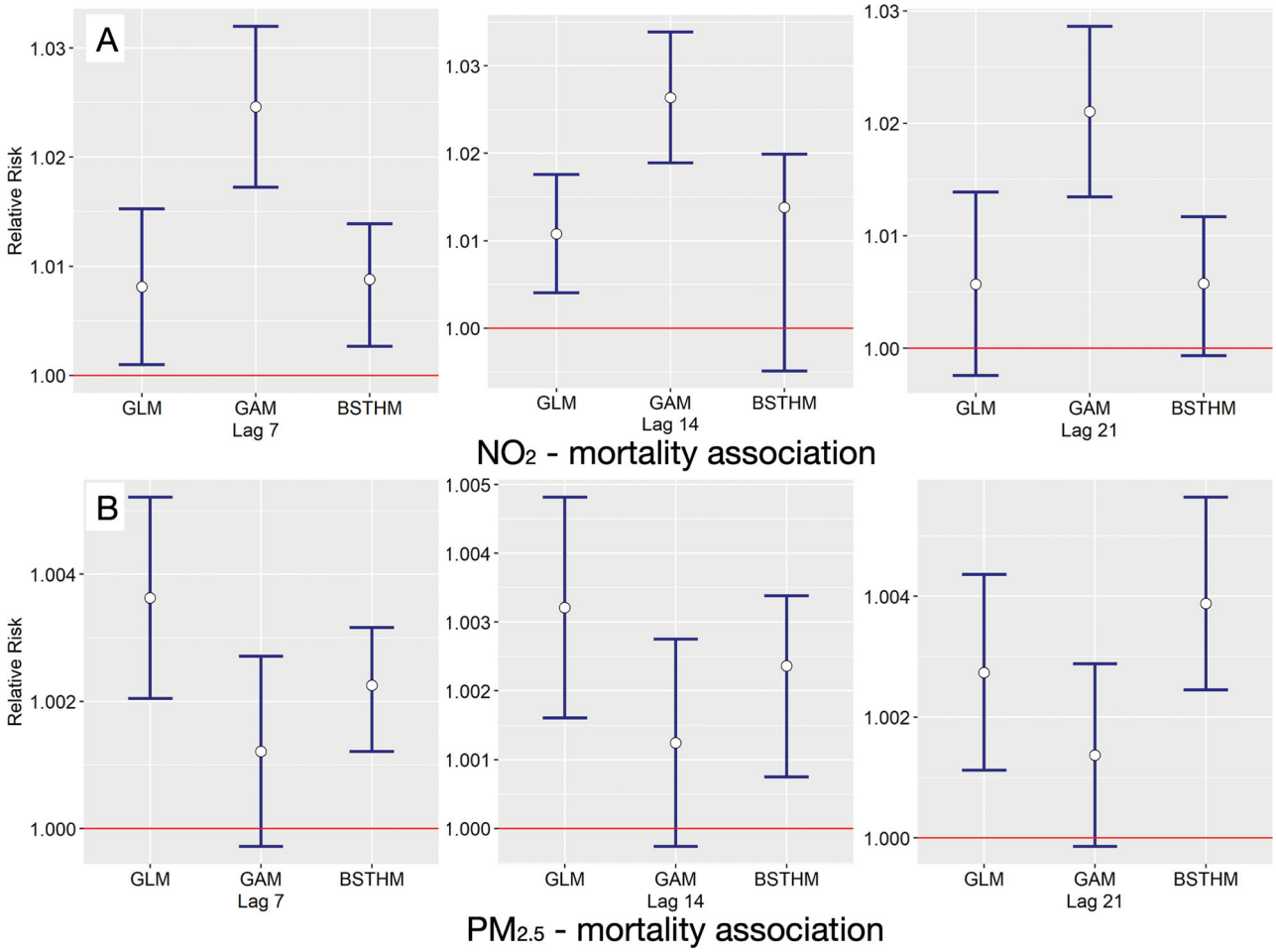

Figure 7. Relative risk (with 95 percent confidence interval) comparison of (A) NO_2 and (B) $PM_{2.5}$ among GLM, GAM, and BSTHM. GLM = generalized linear model; GAM = generalized additive model; BSTHM = Bayesian space–time hierarchical model.

Generally, overall positive trends are revealed with the lag effects of seven, fourteen, and twenty-one days. For the NO_2–mortality association, the relative risks of 1.008 (CI [1.008, 1.015]), 1.011 (CI [1.004, 1.018]), and 1.006 (CI [0.998, 1.014]) are shown with seven-, fourteen-, and twenty-one-day lag effects using GLM. Using GAM, the RRs of 1.025 (CI [1.017, 1.032]), 1.026 (CI [1.019, 1.034]), and 1.021 (CI [1.013, 1.029]) are estimated for NO_2 under different time lag effects. The relative risks of BSTHM, as reported earlier, had values of 1.009 (CI [1.003, 1.014]), 1.014 (CI [0.995, 1.02]), and 1.006 (CI [0.999, 1.012]) under each lag effect scenario. For the $PM_{2.5}$–mortality association, the RRs of GLM, GAM, and BSTHM are 1.004 (CI [1.002, 1.005]), 1.001 (CI [0.999, 1.003]), and 1.002 (CI [1.001, 1.003]) under the seven-day lag effect; 1.003 (CI [1.002, 1.005]), 1.001 (CI [0.999, 1.003]), and 1.002 (CI [1.001, 1.003]) under the fourteen-day lag effect; and 1.003 (CI [1.001, 1.004]), 1.001 (CI [0.999, 1.003]), and 1.004 (CI [1.002, 1.006]) under the twenty-one-day lag effect.

Based on the relative risk estimation in Figure 7, one can see that different lag effects including seven, fourteen, and twenty-one days reveal limited impacts on the RR variation. Discrepancies are mainly caused by different models. Compared with GLM and BSTHM, GAM shows higher relative risks of NO_2 with different lag effects. Similar RR patterns of NO_2 are revealed using GLM and BSTHM, which are all lower than the RRs of GAM. For the RRs of $PM_{2.5}$, lag effects of seven and fourteen days show similar RR patterns, with GLM exhibiting the highest risks and GAM yielding the lowest risks. Differences are shown in the lag effect of twenty-one days, with BSTHM reporting the highest risk compared with GAM and GLM. Although discrepancies are found among different models, which are consistent with the model evaluation in Table 4, the overall risk trends based on GLM, GAM, and BSTHM

are similar, revealing the reliability of the proposed model for risk estimation.

Discussion

Although studies of air pollution and epidemic diseases have benefited from existing research that considers multiperspective physical and socioeconomic factors (Silva et al. 2017; Rahimi et al. 2021; Srivastava 2021), the local spatial variations of air pollution–COVID-19 interactions has not been well-studied. This study explored the association between daily air pollutants, including NO_2 and $PM_{2.5}$, and COVID-19 mortality between 1 April and 31 December. The epidemiological analysis focuses on the RRs of NO_2 and $PM_{2.5}$ to the changes of daily deaths based on a global scale and individual cities.

The results are consistent with previous studies that show that higher NO_2 and $PM_{2.5}$ emissions are associated with increased deaths caused by respiratory diseases (Wu et al. 2020; Zoran et al. 2020). Liu et al. (2019) reported the independent association between short-term exposure to $PM_{2.5}$ and daily respiratory diseases in more than 600 cities on a global scale. Moreover, Villeneuve and Goldberg (2020) provided a literature review on ambient air pollution and the increased risk of severe acute respiratory syndrome and COVID-19, with all studies reporting positive associations. In addition, long-term exposure to NO_2 and $PM_{2.5}$ was explored by Zhang et al. (2021), who found a positive association with the increasing risks of respiratory mortality.

It should be noted that despite the positive trends on a global scale, several individual cities in this study showed a negative association between NO_2, $PM_{2.5}$, and COVID-19 mortality, which is opposite to the overall global trends. The findings reveal the impact of multiple spatial scales on estimating air pollution risks. Previous studies have discussed the influence of multiscale air pollution on public health, involving both scales and boundary districts (Thompson and Selin 2012; Markakis et al. 2014). Butt et al. (2017) analyzed the influence of $PM_{2.5}$ in several regions on the changes of global attributable deaths, indicating that the increasing global population- weighted $PM_{2.5}$ was mainly dominated by the increase in China and India. Research by Thompson and Selin (2012) evaluated the uncertainty of air quality and health impacts based on different scales, showing the variation of ozone concentration at 36-, 12-, 4-, and 2-km resolution. Those discrepancies in RRs were also discussed earlier. The changes in COVID-19 mortality, the level of air pollution, and human mobility variation in individual cities are considered to discuss the RR discrepancies. For instance, a smaller number of total deaths, lower level air pollution, and higher level human mobility variation could lead to biases in RR estimation. The RR patterns in several cities, such as Providence and Wayne in the United States, however, were not explained by these factors. This reveals the fact that compared with the classic risk factors, short-term exposure to air pollution shows a lower impact on health conditions that could lead to the nonpositive associations (Liu et al. 2019).

This study has a few new findings. First, it provides evidence on potential risks of air pollution exposure under the scenario of lockdown and restricted social distancing policies before vaccination. Second, both global and city-level analyses were investigated and compared to illustrate the impact of multiscale variation on risk estimation of air pollution. This research reinforces the evidence of the discrepancies of linkages between daily NO_2, $PM_{2.5}$, and COVID-19 mortality on the city scale and global scale.

There are also some limitations of this study. First, cities selected in this study are limited due to the availability of multisourced daily data. For instance, cities that lack ground-level air pollution data were excluded from this study. Air pollution exposure estimation based on the integration of ground-level and satellite-level air pollution data is not considered in this study because of the biases on the fine-scale daily data estimation (Sullivan and Krupnick 2018). Thus, the coverage of the collected data might be not representative to estimate the air pollutants–COVID-19 mortality on a complete global scale. Moreover, although the overall trends of air pollution risks among models were assessed, the discrepancies in RRs caused by GLM, GAM, and BSTHM in individual cities were not discussed. Evidence of estimation biases could be provided by comparing individual city-level relative risks of NO_2 and $PM_{2.5}$. For instance, by comparing the RRs of $PM_{2.5}$ using GLM and GAM in individual cities, the negative association trends in Providence in the United States estimated by BSTHM could be further evaluated.

Conclusion

Understanding the association between multiscale air pollution and COVID-19 mortality is significant in finding the potential factors that could increase the severity of COVID-19 infections. This study provided a global perspective of the ground-level daily NO_2 and $PM_{2.5}$ between 1 April and 31 December 2020 and estimated multiscale RRs of these air pollutants accounting for the meteorological and human mobility factors using a BSTHM model.

Results suggested a significant relationship between daily ground-level air pollutants and COVID-19 mortality based on BSTHM. With the lag effects of seven, fourteen, and twenty-one days, the RRs of NO_2 and $PM_{2.5}$, ranging from 1.006 to 1.014 and from 1.002 to 1.004, respectively, are higher with the increasing number of daily deaths. Moreover, variations in RRs are shown among individual cities. RRs of NO_2 based on seven-, fourteen-, and twenty-one-day lag effects are between 0.754 and 1.138, between 0.973 and 1.245, and between 0.935 and 1.141, respectively, whereas the RRs of $PM_{2.5}$ range from 0.888 to 1.032, from 0.968 to 1.013, and from 0.971 to 1.023 with the lag effects of seven, fourteen, and twenty-one days, respectively. Findings reveal the discrepancies in assessing air pollution in individual cities compared with global analysis, exhibiting the need to investigate the potential impact of the multiscale spatial effect of global air pollution on COVID-19 mortality.

Funding

We are grateful for funding support from grants by the General Research Fund (Grant Nos. 15602619, 15603920, 14605920, 14611621) and the Collaborative Research Fund (Grant Nos. C7064-18GF, C4023-20GF) from the Hong Kong Research Grants Council, the project 1-CD81 from the Research Institute for Land and Space of the Hong Kong Polytechnic University, and the Research Committee on Research Sustainability of Major Research Grants Council Funding Schemes of the Chinese University of Hong Kong.

ORCID

Yuan Meng http://orcid.org/0000-0002-0963-0581
Man Sing Wong http://orcid.org/0000-0002-6439-6775
Mei-Po Kwan http://orcid.org/0000-0001-8602-9258
Rui Zhu http://orcid.org/0000-0002-9965-0948

References

Akimoto, H. 2003. Global air quality and pollution. *Science* 302 (5651):1716–19. doi: 10.1126/science.1092666.

Andrée, B. P. J. 2020. *Incidence of COVID-19 and connections with air pollution exposure: Evidence from the Netherlands*. Washington, DC: The World Bank.

Barnett-Itzhaki, Z., and A. Levi. 2021. Effects of chronic exposure to ambient air pollutants on COVID-19 morbidity and mortality—A lesson from OECD countries. *Environmental Research* 195:110723. doi: 10.1016/j.envres.2021.110723.

Bashir, M. F., B. Ma, B. Komal, M. A. Bashir, D. Tan, and M. Bashir. 2020. Correlation between climate indicators and COVID-19 pandemic in New York, USA. *Science of the Total Environment* 728:138835. doi: 10.1016/j.scitotenv.2020.138835.

Besag, J., J. York, and A. Mollié. 1991. Bayesian image restoration, with two applications in spatial statistics. *Annals of the Institute of Statistical Mathematics* 43 (1):1–20. doi: 10.1007/BF00116466.

Bishop, G., and G. Welch. 2001. An introduction to the Kalman filter. *Proceedings of SIGGRAPH, Course* 8 (41):27599–23175.

Brunekreef, B., and S. T. Holgate. 2002. Air pollution and health. *The Lancet* 360 (9341):1233–42. doi: 10.1016/S0140-6736(02)11274-8.

Butt, E., S. Turnock, R. Rigby, C. Reddington, M. Yoshioka, J. Johnson, L. Regayre, K. Pringle, G. Mann, and D. Spracklen. 2017. Global and regional trends in particulate air pollution and attributable health burden over the past 50 years. *Environmental Research Letters* 12 (10):104017. doi: 10.1088/1748-9326/aa87be.

Chang, S., E. Pierson, P. W. Koh, J. Gerardin, B. Redbird, D. Grusky, and J. Leskovec. 2021. Mobility network models of COVID-19 explain inequities and inform reopening. *Nature* 589 (7840):82–87. doi: 10.1038/s41586-020-2923-3.

Chen, R., H. Kan, B. Chen, W. Huang, Z. Bai, G. Song, and G. Pan, CAPES Collaborative Group. 2012. Association of particulate air pollution with daily mortality: The China Air Pollution and Health Effects Study. *American Journal of Epidemiology* 175 (11):1173–81. doi: 10.1093/aje/kwr425.

Chinazzi, M., J. T. Davis, M. Ajelli, C. Gioannini, M. Litvinova, S. Merler, A. Pastore, Y. Piontti, K. Mu, L. Rossi, et al. 2020. The effect of travel restrictions on the spread of the 2019 novel coronavirus (COVID-19) outbreak. *Science* 368 (6489):395–400. doi: 10.1126/science.aba9757.

Chowkwanyun, M., and A. L. Reed, Jr. 2020. Racial health disparities and COVID-19—Caution and

context. *New England Journal of Medicine* 383 (3):201–3. doi: 10.1056/NEJMp2012910.

Chu, D. K., E. A. Akl, S. Duda, K. Solo, S. Yaacoub, H. J. Schünemann, D. K. Chu, E. A. Akl, A. El-Harakeh, A. Bognanni, et al. 2020. Physical distancing, face masks, and eye protection to prevent person-to-person transmission of SARS-CoV-2 and COVID-19: A systematic review and meta-analysis. *The Lancet* 395 (10242):1973–87. doi: 10.1016/S0140-6736(20)31142-9.

Coccia, M. 2020. Factors determining the diffusion of COVID-19 and suggested strategy to prevent future accelerated viral infectivity similar to COVID. *Science of the Total Environment* 729:138474. doi: 10.1016/j.scitotenv.2020.138474.

Coccia, M. 2021. The effects of atmospheric stability with low wind speed and of air pollution on the accelerated transmission dynamics of COVID-19. *International Journal of Environmental Studies* 78 (1):1–27. doi: 10.1080/00207233.2020.1802937.

Di, Q., L. Dai, Y. Wang, A. Zanobetti, C. Choirat, J. D. Schwartz, and F. Dominici. 2017. Association of short-term exposure to air pollution with mortality in older adults. *JAMA* 318 (24):2446–56. doi: 10.1001/jama.2017.17923.

Dunson, D. B. 2001. Commentary: Practical advantages of Bayesian analysis of epidemiologic data. *American Journal of Epidemiology* 153 (12):1222–26. doi: 10.1093/aje/153.12.1222.

Forster, P. M., H. I. Forster, M. J. Evans, M. J. Gidden, C. D. Jones, C. A. Keller, R. D. Lamboll, C. L. Quéré, J. Rogelj, D. Rosen, et al. 2020. Current and future global climate impacts resulting from COVID-19. *Nature Climate Change* 10 (10):913–19. doi: 10.1038/s41558-020-0883-0.

Giani, P., S. Castruccio, A. Anav, D. Howard, W. Hu, and P. Crippa. 2020. Short-term and long-term health impacts of air pollution reductions from COVID-19 lockdowns in China and Europe: A modelling study. *The Lancet Planetary Health* 4 (10):e474–82. doi: 10.1016/S2542-5196(20)30224-2.

Gujral, H., and A. Sinha. 2021. Association between exposure to airborne pollutants and COVID-19 in Los Angeles, United States with ensemble-based dynamic emission model. *Environmental Research* 194:110704.

He, G., Y. Pan, and T. Tanaka. 2020. The short-term impacts of COVID-19 lockdown on urban air pollution in China. *Nature Sustainability* 3 (12):1005–11. doi: 10.1038/s41893-020-0581-y.

He, K., H. Huo, and Q. Zhang. 2002. Urban air pollution in China: Current status, characteristics, and progress. *Annual Review of Energy and the Environment* 27 (1):397–431. doi: 10.1146/annurev.energy.27.122001.083421.

Huang, J., and M.-P. Kwan. 2021. Uncertainties in the assessment of COVID-19 risk: A study of people's exposure to high-risk environments using individual-level activity data. *Annals of the American Association of Geographers*. Advance online publication. doi: 10.1080/24694452.2021.1943301.

Huang, J., M.-P. Kwan, and Z. Kan. 2021. The super-spreading places of COVID-19 and the associated built-environment and socio-demographic features: A study using a spatial network framework and individual-level activity data. *Health & Place* 72:102694. doi: 10.1016/j.healthplace.2021.102694.

Kan, Z., M.-P. Kwan, M. S. Wong, J. Huang, and D. Liu. 2021. Identifying the space–time patterns of COVID-19 risk and their associations with different built environment features in Hong Kong. *The Science of the Total Environment* 772 (10):145379. doi: 10.1016/j.scitotenv.2021.145379.

Khomenko, S., M. Cirach, E. Pereira-Barboza, N. Mueller, J. Barrera-Gómez, D. Rojas-Rueda, K. de Hoogh, G. Hoek, and M. Nieuwenhuijsen. 2021. Premature mortality due to air pollution in European cities: A health impact assessment. *The Lancet. Planetary Health* 5 (3):e121–34. doi: 10.1016/S2542-5196(20)30272-2.

Knorr-Held. L. 2000. Bayesian modelling of inseparable space–time variation in disease risk. *Statistics in Medicine* 19 (17–18):2555–67. doi: 10.1002/1097-0258(20000915/30)19:17/18<2555::AID-SIM587>3.0.CO;2-#.

Kwok, C. Y. T., M. S. Wong, K. L. Chan, M.-P. Kwan, J. E. Nichol, C. H. Liu, J. Y. H. Wong, A. K. C. Wai, L. W. C. Chan, Y. Xu, et al. 2021. Spatial analysis of the impact of urban geometry and socio-demographic characteristics on COVID-19, a study in Hong Kong. *Science of the Total Environment* 764:144455. doi: 10.1016/j.scitotenv.2020.144455.

Le Quéré, C., R. B. Jackson, M. W. Jones, A. J. P. Smith, S. Abernethy, R. M. Andrew, A. J. De-Gol, D. R. Willis, Y. Shan, J. G. Canadell, et al. 2020. Temporary reduction in daily global CO_2 emissions during the COVID-19 forced confinement. *Nature Climate Change* 10 (7):647–53. doi: 10.1038/s41558-020-0797-x.

Lelieveld, J., J. S. Evans, M. Fnais, D. Giannadaki, and A. Pozzer. 2015. The contribution of outdoor air pollution sources to premature mortality on a global scale. *Nature* 525 (7569):367–71. doi: 10.1038/nature15371.

Li, J., J. Wang, N. Wang, and H. Li. 2018. A Bayesian space–time hierarchical model for remotely sensed lattice data based on multiscale homogeneous statistical units. *IEEE Journal of Selected Topics in Applied Earth Observations and Remote Sensing* 11 (7):2151–61. doi: 10.1109/JSTARS.2018.2818286.

Li, J., N. Wang, J. Wang, and H. Li. 2018. Spatiotemporal evolution of the remotely sensed global continental $PM_{2.5}$ concentration from 2000–2014 based on Bayesian statistics. *Environmental Pollution* 238:471–81. doi: 10.1016/j.envpol.2018.03.050.

Li, S., S. Ma, and J. Zhang. 2021. Association of built environment attributes with the spread of COVID-19 at its initial stage in China. *Sustainable Cities and Society* 67:102752. doi: 10.1016/j.scs.2021.102752.

Liao, J., Z. Qin, Z. Zuo, S. Yu, and J. Zhang. 2016. Spatial-temporal mapping of hand foot and mouth disease and the long-term effects associated with climate and socio-economic variables in Sichuan Province, China from 2009 to 2013. *Science of the Total Environment* 563–564:152–59. doi: 10.1016/j.scitotenv.2016.03.159.

Liu, C., R. Chen, F. Sera, A. M. Vicedo-Cabrera, Y. Guo, S. Tong, M. S. Z. S. Coelho, P. H. N. Saldiva, E. Lavigne, P. Matus, et al. 2019. Ambient particulate air pollution and daily mortality in 652 cities. *The New England Journal of Medicine* 381 (8):705–15. doi: 10.1056/NEJMoa1817364.

Ma, Y., Y. Zhao, J. Liu, X. He, B. Wang, S. Fu, J. Yan, J. Niu, J. Zhou, and B. Luo. 2020. Effects of temperature variation and humidity on the death of COVID-19 in Wuhan, China. *The Science of the Total Environment* 724:138226. doi: 10.1016/j.scitotenv.2020.138226.

Markakis, K., M. Valari, A. Colette, O. Sanchez, O. Perrussel, C. Honore, R. Vautard, Z. Klimont, and S. Rao. 2014. Air quality in the mid-21st century for the city of Paris under two climate scenarios: From the regional to local scale. *Atmospheric Chemistry and Physics* 14 (14):7323–40. doi: 10.5194/acp-14-7323-2014.

Mathieu, E., H. Ritchie, E. Ortiz-Ospina, M. Roser, J. Hasell, C. Appel, C. Giattino, and L. Rodés-Guirao. 2021. A global database of COVID-19 vaccinations. *Nature Human Behaviour* 5:947–53. doi: 10.1038/s41562-021-01122-8.

Meng, Y., M. S. Wong, H. Xing, R. Zhu, K. Qin, M.-P. Kwan, K. H. Lee, C. Y. T. Kwok, and H. Li. 2021. Effects of urban functional fragmentation on nitrogen dioxide (NO_2) variation with anthropogenic-emission restriction in China. *Scientific Reports* 11 (1):1–15. doi: 10.1038/s41598-021-91236-w.

Ming, W., Z. Zhou, H. Ai, H. Bi, and Y. Zhong. 2020. COVID-19 and air quality: Evidence from China. *Emerging Markets Finance and Trade* 56 (10):2422–42. doi: 10.1080/1540496X.2020.1790353.

Ogen, Y. 2020. Assessing nitrogen dioxide (NO_2) levels as a contributing factor to the coronavirus (COVID-19) fatality rate. *Science of the Total Environment* 726:138605. doi: 10.1016/j.scitotenv.2020.138605.

Oyedotun, T. D. T., and S. Moonsammy. 2021. Spatiotemporal variation of COVID-19 and its spread in South America: A rapid assessment. *Annals of the American Association of Geographers* 111 (6):1868–79.

Prata, D. N., W. Rodrigues, and P. H. Bermejo. 2020. Temperature significantly changes COVID-19 transmission in (sub)tropical cities of Brazil. *Science of the Total Environment* 729:138862. doi: 10.1016/j.scitotenv.2020.138862.

Rahimi, N. R., R. Fouladi-Fard, R. Aali, A. Shahryari, M. Rezaali, Y. Ghafouri, M. R. Ghalhari, M. Asadi-Ghalhari, B. Farzinnia, O. Conti Gea, et al. 2021. Bidirectional association between COVID-19 and the environment: A systematic review. *Environmental Research* 194:110692. doi: 10.1016/j.envres.2020.110692.

Richardson, S., J. J. Abellan, and N. Best. 2006. Bayesian spatio-temporal analysis of joint patterns of male and female lung cancer risks in Yorkshire (UK). *Statistical Methods in Medical Research* 15 (4):385–407. doi: 10.1191/0962280206sm458oa.

Sarkodie, S. A., and P. A. Owusu. 2020. Impact of meteorological factors on COVID-19 pandemic: Evidence from top 20 countries with confirmed cases. *Environmental Research* 191:110101. doi: 10.1016/j.envres.2020.110101.

Shan, Y., J. Ou, D. Wang, Z. Zeng, S. Zhang, D. Guan, and K. Hubacek. 2021. Impacts of COVID-19 and fiscal stimuli on global emissions and the Paris Agreement. *Nature Climate Change* 11 (3):200–07. doi: 10.1038/s41558-020-00977-5.

Shao, W., J. Xie, and Y. Zhu. 2021. Mediation by human mobility of the association between temperature and COVID-19 transmission rate. *Environmental Research* 194:110608. doi: 10.1016/j.envres.2020.110608.

Silva, R. A., J. J. West, J.-F. Lamarque, D. T. Shindell, W. J. Collins, G. Faluvegi, G. A. Folberth, L. W. Horowitz, T. Nagashima, V. Naik, et al. 2017. Future global mortality from changes in air pollution attributable to climate change. *Nature Climate Change* 7 (9):647–51. doi: 10.1038/nclimate3354.

Srivastava, A. 2021. COVID-19 and air pollution and meteorology—An intricate relationship: A review. *Chemosphere* 263:128297. doi: 10.1016/j.chemosphere.2020.128297.

Sullivan, D. M., and A. Krupnick. 2018. Using satellite data to fill the gaps in the U.S. air pollution monitoring network. Resources for the Future Working Paper 18-21, Washington, DC.

Thompson, T. M., and N. E. Selin. 2012. Influence of air quality model resolution on uncertainty associated with health impacts. *Atmospheric Chemistry and Physics* 12 (20):9753–62. doi: 10.5194/acp-12-9753-2012.

Travaglio, M., Y. Yu, R. Popovic, L. Selley, N. S. Leal, and L. M. Martins. 2021. Links between air pollution and COVID-19 in England. *Environmental Pollution* 268 (Pt A):115859. doi: 10.1016/j.envpol.2020.115859.

Venter, Z. S., K. Aunan, S. Chowdhury, and J. Lelieveld. 2020. COVID-19 lockdowns cause global air pollution declines. *Proceedings of the National Academy of Sciences of the United States of America* 117 (32):18984–90. doi: 10.1073/pnas.2006853117.

Villeneuve, P. J., and M. S. Goldberg. 2020. Methodological considerations for epidemiological studies of air pollution and the SARS and COVID-19 coronavirus outbreaks. *Environmental Health Perspectives* 128 (9):95001. doi: 10.1289/EHP7411.

Wang, Z., Y. Yue, B. He, K. Nie, W. Tu, Q. Du, and Q. Li. 2021. A Bayesian spatio-temporal model to analyzing the stability of patterns of population distribution in an urban space using mobile phone data. *International Journal of Geographical Information Science* 35 (1):116–34. doi: 10.1080/13658816.2020.1798967.

Weiss, D. J., A. Nelson, C. A. Vargas-Ruiz, K. Gligorić, S. Bavadekar, E. Gabrilovich, A. Bertozzi-Villa, J. Rozier, H. S. Gibson, T. Shekel, et al. 2020. Global maps of travel time to healthcare facilities. *Nature Medicine* 26 (12):1835–38. doi: 10.1038/s41591-020-1059-1.

Wu, X., R. C. Nethery, M. B. Sabath, D. Braun, and F. Dominici. 2020. Air pollution and COVID-19 mortality in the United States: Strengths and limitations of an ecological regression analysis. *Science Advances* 6 (45): eabd4049.

Xie, J., and Y. Zhu. 2020. Association between ambient temperature and COVID-19 infection in 122 cities from China. *Science of the Total Environment* 724:138201. doi: 10.1016/j.scitotenv.2020.138201.

Yancy, C. W. 2020. COVID-19 and African Americans. *JAMA* 323 (19):1891–92. doi: 10.1001/jama.2020.6548.

Zhai, W., M. Liu, X. Fu, and Z.-R. Peng. 2021. American inequality meets COVID-19: Uneven spread of the disease across communities. *Annals of the American Association of Geographers* 111:1–21. doi: 10.1080/24694452.2020.1866489.

Zhang, Z., J. Wang, J. C. Kwong, R. T. Burnett, A. van Donkelaar, P. Hystad, R. V. Martin, L. Bai, J. McLaughlin, and H. Chen. 2021. Long-term exposure to air pollution and mortality in a prospective cohort: The Ontario Health Study. *Environment International* 154:106570. doi: 10.1016/j.envint.2021.106570.

Zhu, Y., J. Xie, F. Huang, and L. Cao. 2020a. Association between short-term exposure to air pollution and COVID-19 infection: Evidence from China. *Science of the Total Environment* 727:138704. doi: 10.1016/j.scitotenv.2020.138704.

Zhu, Y., J. Xie, F. Huang, and L. Cao. 2020b. The mediating effect of air quality on the association between human mobility and COVID-19 infection in China. *Environmental Research* 189:109911. doi: 10.1016/j.envres.2020.109911.

Zoran, M. A., R. S. Savastru, D. M. Savastru, and M. N. Tautan. 2020. Assessing the relationship between surface levels of PM2. 5 and PM10 particulate matter impact on COVID-19 in Milan, Italy. *Science of the Total Environment* 738:139825. doi: 10.1016/j.scitotenv.2020.139825.

YUAN MENG is a PhD Candidate in the Department of Land Surveying and Geo-Informatics, the Hong Kong Polytechnic University, Kowloon, Hong Kong, China. E-mail: myuan.meng@connect.polyu.hk. Her research interests include the spatial analysis of land use and land cover, urban built-up environment, and public health.

MAN SING WONG is a Professor in the Department of Land Surveying and Geo-Information, the Hong Kong Polytechnic University, Kowloon, Hong Kong, China. E-mail: Ls.charles@polyu.edu.hk. His research interests include GIScience, urban remote sensing, and geospatial health study.

MEI-PO KWAN is Choh-Ming Li Professor of Geography and Resource Management and Director of the Institute of Space and Earth Information Science at the Chinese University of Hong Kong, Shatin, Hong Kong, China. E-mail: mpk654@gmail.com. Her research interests include environmental health, human mobility, sustainable cities, transport and health issues in cities, and GIScience.

RUI ZHU is a Research Assistant Professor in the Department of Land Surveying and Geo-Information, The Hong Kong Polytechnic University, Kowloon, Hong Kong, China. E-mail: felix.zhu@polyu.edu.hk. His research interests include geo-public health, solar cities, urban heat islands, and smart mobility.